Reconfigurable Intelligent Surfaces for Downlink Cellular Networks

Phuc Quang Truong(✉) and Ca Phan Van

Ho Chi Minh City University of Technology and Education,
Ho Chi Minh City, Vietnam
{phuctq,capv}@hcmute.edu.vn

Abstract. In this work, we propose a joint optimization of power allocation and phase shift for downlink RIS-aided cellular networks. In particular, the total network throughput was maximized under power consumption and QoS constraints. To tackle this problem, we consider power allocation procedure to solve the convex problem of power control coefficients optimization and Block Coordinate Descent (BCD)-based procedure to solve non-convex problem of RIS phase shift optimization. The numerical results are provided to illustrate the effectiveness of the proposed approach in terms of enhancing the coverage and the total network throughput.

Keywords: Reconfigurable intelligent surfaces · Power allocation · Phase shift optimization · Cellular network · Convex optimization

1 Introduction

Reconfigurable Intelligent Surfaces (RISs) are man-made panels that can be capable of configuring the properties of impinging electromagnetic waves based on Snell's law. RIS is the key technology enabling the 6th generation (6G) in the near future. With highlight features, RISs can work without energy source in case of reflecting incident signal only. Different from relaying or decoding and forwarding, RISs can response full-band and nearly not be affected by receiver noise [1]. Due to the potential advantages, RISs are not only the conceptual research but also they are deployed in practical scenarios [2]. The numerical results in [3] prove that RIS-aided wireless communication networks can achieve higher performance than traditional wireless networks.

In [4], the authors assumed the RIS-aided single cell wireless system with multi antennas at the access point (AP) and single antenna at K users. The RIS is equipped with N reflected elements which are controlled by the RIS-controller to switch either receiving mode or reflecting mode. In this case, the total transmit power at the AP is minimized by combining optimizing both active beamforming at the AP and passive beamforming with the user signal-to-interference-plus-noise ratio (SINR) constraints. To tackle this problem, both the semidefinite

Supported by Ho Chi Minh City University of Technology and Education, Vietnam.

N.-S. Vo et al. (Eds.): INISCOM 2022, LNICST 444, pp. 20–32, 2022.
https://doi.org/10.1007/978-3-031-08878-0_2

relaxation (SDR) and alternating optimization algorithms were applied. On the other hand, RIS-aided the wireless network including a base station (BS) with M antennas and K single-antenna users worked in two scenarios: multicasting and multi-user downlink communication. The authors proposed alternating direction method of multipliers (ADMM) algorithm to maximize the smallest signal-to-noise ratio (SNR) in passive beamforming problem [5].

In [6], the authors developed algorithm of low computational complexity to maximize the worst rate subject to the transmit power constraints by jointly designing the reflecting coefficient of RISs and transmit beamformers. In particular, the network of a multiple antenna AP transmitting to multiple single-antenna users, under both proper Gaussian signaling and improper Gaussian signaling with RIS-aided communication in case of without direct link from AP to users.

Recently, RIS-assisted unmanned aerial vehicle (UAV) communication becomes the promising technique to enhance the quality of communication. The scenario in [7] investigated a communication system consisting of a UAV, a ground user, and a RIS on building. Jointly UAV trajectory and passive beamforming at RIS were applied to maximize the average achievable rate of system. Furthermore, the application of UAV becomes more widen in numerous fields such as surveillance, disaster rescue mission, and geography exploration. Hence, the performance network and the quality of service need to enhance and ensure the connection between UAVs and users. In these cases, RIS-assisted multi-UAV networks plays an important role in supporting the connection from UAVs to users when the link is blocked by obstacles. In [8], deep reinforcement learning (DRL) approach was investigated to solve the continuous optimization problem that aimed to maximize the energy efficiency of UAVs networks. Similarly, DRL approach was proposed to maximize the network sum-rate in device-to-device (D2D) communications supported by RIS in [9].

Due to the significant benefits of both spectral efficiency and energy efficiency, non-orthogonal multiple access (NOMA) is the potential technique for future communication networks such as the beyond fifth-generation (B5G), 6G [10]. Thus, the combination of NOMA and RIS will help to enhance the coverage and energy efficiency. Particularly, an RIS-NOMA multi-input-single-output (MISO) system was investigated in [11] to maximize the sum-rate and minimize the total power consumption. To tackle this, the alternating successive convex approximation (SCA) and SDR based algorithms were proposed to solve the jointly transmit beamforming at the BS and passive beamforming at the RIS problems. In [12], the authors assumed that RIS-assisted the wireless power communication network to ensure the connection between a single-antenna BS and single-antenna users. To maximizing the throughput of the network, the authors combined optimizing the reflect beamforming of RIS and the time allocation for power transfer and information transmission BS and users in case of NOMA and time division multiple access (TDMA).

The multi RIS-assisted wireless network including a multi antennas AP and two groups of single antenna users was investigated in [13]. The authors aimed to minimize the transmit power at AP with the individual SINR constraint on information and energy harvesting at energy users.

In [14–16], the authors aimed to maximize the weighted sum rate at all users and the weighted sum power in a RIS-assisted wireless communication system via jointly optimizing the active beamforming at the transmitter and the reflect phase shift at the RISs. Nevertheless, the formulated problems are non-convex. Hence, in [16] the authors based on the fractional programming method to optimize active beamforming at BS and three low-complexity algorithms to solve the passive beamforming problem. Meanwhile, in [14] the authors utilized the sequential rank-one constraint relaxation approach to tackle the passive beamforming problem.

The main contributions of this work focus on extending coverage of the cellular networks by proposing the RIS technology to enhance the reliable of wireless networks, meanwhile the number of users increases rapidly. In particular, to tackle this problem, the joint power allocation at BS and phase shift optimization has been solved by both power allocation procedure in Algorithm 1 and BCD-based procedure in Algorithm 2.

The rest of the paper is organized as follows. We explain the system model of the proposed RIS-assisted downlink cellular network in Sect. 2. Meanwhile, Sect. 3 and Sect. 4 develop the problem statement, methodology and the joint power allocation and phase shift optimization, respectively. The simulation results are discussed in Sect. 5. Finally, the conclusion of the paper is provided in Sect. 6.

2 System Model

2.1 Network Model

In cellular networks, many user equipments (UEs) receive poor signal's quality from the BS because of shadowing and blocking effect. As illustrated in Fig. 1, we study the issue of throughput enhancement for downlink cellular networks with the assistance of RISs panels. Specifically, we assume that the UEs are devided into M groups. And they are uniform randomly distributed in the coverage area. The set of UEs and the group of users are denoted as $\mathcal{K} = \{1, ..., K\}$ and $\mathcal{M} = \{1, ..., M\}$, respectively. The UEs are equipped with a single antenna.

The RISs are installed on the top of buildings, to work as small cell BS where each RIS is consisted of N elements. The m-th group can cover a limited number of UEs, $\mathcal{K}_m = \{1, ..., K_m\}$ for $m \in \mathcal{M}$. The (m, k)-th UE demonstrates the k-th user in the m-th group.

The aim of this paper is to maximize the total throughput of cellular networks by exploiting the RIS technology to extend the coverage of wireless network and to serve many UEs with high QoS.

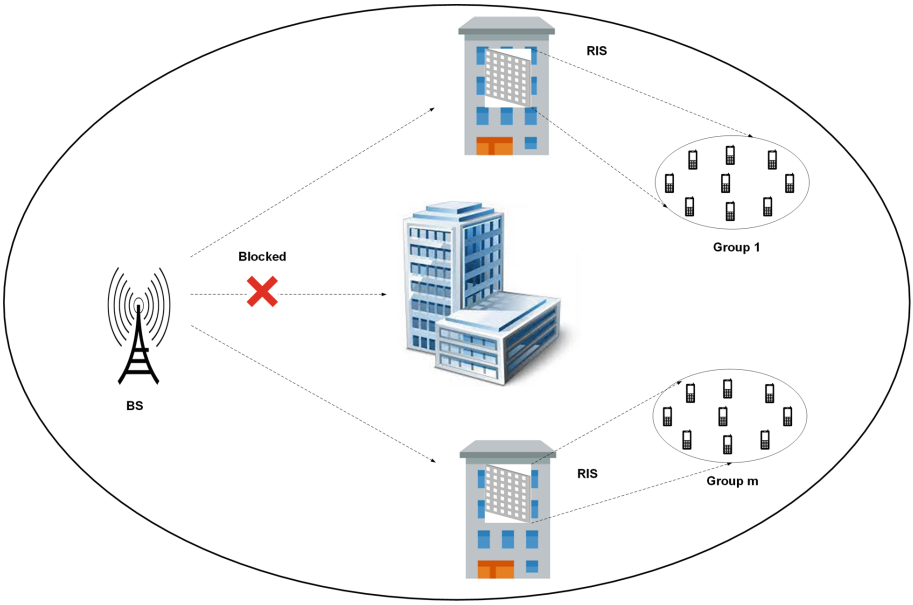

Fig. 1. An illustration of downlink RIS-aided cellular communications.

2.2 RIS-Aided Communication Models

To consider the assistance of RIS in communication models, we investigate the coordinate of the BS, the RISs and of all UEs as (x_0, y_0, H_0), (x_m, y_m, H_m), $m \in \mathcal{M}$ and $(x_k, y_k, 0)$, $k \in \mathcal{K}$, where H_0 and H_m denote the height of the BS and the RIS altitude, respectively.

We focus on enhancing the links between the BS and the RISs. Thus, the path loss of the link from the BS to the m-th RIS follows the free-space path loss, i.e., line of sight (LoS), model as [17,18]

$$\beta_{0,m} = \beta_0 R_{0,m}^{-2}, \ m = 1, ..., M, \tag{1}$$

where we denote β_0 as the channel gain at reference position. In addition, $R_{0,m}$ is the distance between the BS and the m-th RIS, which is give by

$$R_{0,m} = \sqrt{d_{0,m}^2 + (H_0 - H_m)^2}, \tag{2}$$

As mention previous, we assign $d_{0,m} = \sqrt{(x_0 - x_m)^2 + (y_0 - y_m)^2}$.

In contrast, a more complicated non-LoS (NLoS) model is applied to the channel from the RIS to the UEs, which is usually affected by shadowing and blockage geometry. Thus, the path loss of the channel from the m-th RIS to the (m,k)-th UE is formulated as [19]

$$\begin{aligned}\beta_{m,k} &= PL_{m,k} + \eta^{LoS} P_{m,k}^{LoS} + \eta^{NLoS} P_{m,k}^{NLoS} \\ &= 10\alpha \log\left(\sqrt{d_{m,k}^2 + H_{U,m}^2}\right) + AP_{m,k}^{LoS} + B, \end{aligned} \tag{3}$$

where η^{LoS} and η^{NLoS} are the average additional losses for LoS and NLoS, respectively, $A = \eta^{LoS} - \eta^{NLoS}$ and $B = 10\alpha \log(\frac{4\pi f_c R_{m,k}}{c}) + \eta^{NLoS}$. The distance path loss is given by

$$PL_{m,k} = 10 \log(\frac{4\pi f_c R_{m,k}}{c})^{\alpha}, \tag{4}$$

We denote f_c and c as carrier frequency in Hz and the speed of light in m/s, respectively. Where $\alpha \geq 2$ is the path loss exponent. The probability of LoS and NLoS is given by [20]

$$P_{m,k}^{LoS} = \frac{1}{1 + a \exp\left[-b\left(\arctan\left(\frac{H_{U,m}}{d_{m,k}}\right) - a\right)\right]}, \tag{5}$$

$$P_{m,k}^{NLoS} = 1 - P_{m,k}^{LoS}, \tag{6}$$

where both a and b are the constants of the environment.

Furthermore, we consider the effect of the phase shift matrix at the m-th RIS $\mathbf{\Phi}_m = diag[\phi_{1m}, \phi_{2m}, ..., \phi_{Nm}]$, here $\phi_{nm} = \alpha_{nm} e^{j\theta_{nm}}$ with $\alpha_{nm} \in [0,1]$ and $\theta_{nm} \in [0, 2\pi]$ $(\forall n = 1, 2, ..., N,\ m \in \mathcal{M})$, that indicates the amplitude of the reflected signal and phase shift of the n-th reflecting element, respectively. We assign $\alpha_{nm} = 1$ because the reflecting element can not change the amplitude of reflecting signals [21]. Under this effect, the small scale fading coefficients, which are assumed as independent and identically distributed random variables with zero mean and unit variance, are used for the link from the BS to m-th RIS and the m-th RIS to the (m,k)-th UE, indicated by $\hat{h}_{0,m} \in \mathbb{C}^{N \times 1}$ and $\hat{h}_{m,k}^H \in \mathbb{C}^{1 \times N}$, respectively. The H is the Hermitian conjugate operation.

Additionally, we denote $\mathbf{h}_{0,m} \in \mathbb{C}^{N \times 1}$ and $\mathbf{h}_{m,k}^H \in \mathbb{C}^{1 \times N}$ as the channel matrix between the BS and the m-th RIS and the m-th RIS to the (m,k)-th UE in the m-th group, respectively. Nevertheless, the cascaded channel matrix of the link between the BS and the (m,k)-th UE through the m-th RIS, $\mathbf{g}_{m,k} \in \mathbb{C}$, can be rewritten as [22]

$$\mathbf{g}_{m,k} = \mathbf{h}_{m,k}^H \mathbf{\Phi}_m \mathbf{h}_{0,m}, \tag{7}$$

where $\mathbf{h}_{0,m} = \sqrt{\beta_{0,m}} \hat{h}_{0,m}$ and $\mathbf{h}_{m,k}^H = \sqrt{\beta_{m,k}} \hat{h}_{m,k}^H$.

2.3 Transmission Schemes

As shown in Fig. 1, the BS transmits signal to its UEs with the reflection from RIS panel deployed on the top of buildings. With TDMA scheme, we have the signal at the k-th UE in the m-th group below

$$y_{m,k} = \sqrt{p_{m,k}}\mathbf{g}_{m,k}s_{m,k} + \ n_k, \tag{8}$$

where $p_{m,k}$ is the transmission power of the BS to the (m,k)-th UE; $s_{m,k}$ is information transmitted by the BS such that $||s_{m,k}||^2 \leq 1$; $n_k \sim \mathcal{CN}(0, \sigma_k^2)$ is the AWGN at the (m,k)-th UE.

Let $\boldsymbol{p}_0 = [\boldsymbol{p}_{0,m}]_{m=1}^{M}$, here $\boldsymbol{p}_{0,m} = [p_{m,k}]_{k=1}^{K_m}$, and $\boldsymbol{\Phi}_M = [\boldsymbol{\Phi}_m]_{m=1}^{M}$ denote the power control coefficients and the phase shifts of RISs, respectively, the received SNR at the (m,k)-th UE can be formulated as

$$\gamma_{m,k}\left(p_{m,k}, \boldsymbol{\Phi}_m\right) = \frac{p_{m,k}\left|\mathbf{g}_{m,k}\right|^2}{\sigma_k^2}. \tag{9}$$

2.4 Information Throughput

The information throughput of the (m,k)-th UE (in bps/Hz) can be expressed as

$$R_{m,k}\left(p_{m,k}, \boldsymbol{\Phi}_m\right) = \log_2\left(1 + \gamma_{m,k}\left(p_{m,k}, \boldsymbol{\Phi}_m\right)\right). \tag{10}$$

Hence, the total throughput of all the UEs in the network can be given by

$$R_{total}\left(\boldsymbol{p}_0, \boldsymbol{\Phi}_M\right) = \sum_{m=1}^{M}\sum_{k=1}^{K_m} R_{m,k}\left(p_{m,k}, \boldsymbol{\Phi}_m\right). \tag{11}$$

3 Problem Statement and Methodology

In this paper, we focus on maximizing the total throughput of downlink cellular networks. To tackle this problem, we jointly optimize $(\boldsymbol{p}_0)$ at the BS and $(\boldsymbol{\Phi}_M)$ of M RISs given some power consumption and QoS constraints. The corresponding optimization problem is as follows:

$$\max_{\boldsymbol{p}_0, \boldsymbol{\Phi}_M} \ R_{total}\left(\boldsymbol{p}_0, \Phi_M\right) \tag{12a}$$

$$\text{s.t.} \quad \sum_{m=1}^{M}\sum_{k=1}^{K_m} p_{m,k} \leq P_0^{\max}, m \in \mathcal{M}, \tag{12b}$$

$$R_{m,k}\left(p_{m,k}, \boldsymbol{\Phi}_m\right) \geq \bar{r}_{m,k}, \ m \in \mathcal{M}, \ k \in \mathcal{K}_m, \tag{12c}$$

$$0 \leq \theta_{nm} \leq 2\pi, \forall n = 1, 2, ..., N, \ m \in \mathcal{M}, \tag{12d}$$

where (12b) is used to limit the total power consumption of all RISs not greater than the maximum transmit power of the BS ($P_0^{\max}$). Meanwhile, (12c) is the QoS constraint at the (m,k)-th UE. And (12d) indicates the lower and upper bounds of the phase shifts when considering the n-th reflecting element of the m-th RIS.

4 Joint Power Allocation and Phase Shift Optimization

It is obvious that the problem (12) is non-convex with the non-convex functions of (12a) and (12c). Therefore, we iteratively optimize the power control coefficients of the BS and the phase shifts of RIS reflecting elements.

4.1 Power Control Coefficients Optimization

For any given $\mathbf{\Phi}_M$, (12) is equivalent to the following power control coefficients optimization problem

$$\max_{\boldsymbol{p}_0} R_{total}\left(\boldsymbol{p}_0\right) \tag{13a}$$

$$\text{s.t.} \quad (12b), (12c). \tag{13b}$$

To solve (13), we utilize the effective approximations and logarithm inequalities [23] based on the property of the convex function $f(z) = \log_2(1+\frac{1}{z}) \geq \hat{f}(z)$, where

$$\hat{f}(z) = \log_2\left(1+\frac{1}{\bar{z}}\right) + \frac{1}{1+\bar{z}} - \frac{z}{(1+\bar{z})\bar{z}}, \tag{14}$$

$\forall z > 0, \bar{z} > 0$. Then, we can write

$$R_{m,k}\left(p_{m,k}\right) \geq \hat{R}^{(i)}_{m,k}\left(p_{m,k}\right), \ \forall k \in \mathcal{K}_m, \ \forall m \in \mathcal{M}, \tag{15}$$

where

$$z = \frac{\sigma_k^2}{p_{m,k}\left|\boldsymbol{g}_{m,k}\right|^2}, \ \bar{z} = z^{(i)} = \frac{\sigma_k^2}{p^{(i)}_{m,k}\left|\boldsymbol{g}_{m,k}\right|^2},$$

$$\hat{R}^{(i)}_{m,k}\left(p_{m,k}\right) = \log_2\left(1+\frac{1}{\bar{z}}\right) + \frac{1}{1+\bar{z}} - \frac{z}{(1+\bar{z})\bar{z}}. \tag{16}$$

So far, (13) can be rewritten as (17) to yield the feasible points at the i-th iteration:

$$\max_{\boldsymbol{p}_0} \hat{R}^{(i)}_{total}\left(\boldsymbol{p}_0\right) \tag{17a}$$

$$\text{s.t.} \quad (12b), \tag{17b}$$

$$\hat{R}^{(i)}_{m,k}\left(\boldsymbol{p}_0\right) \geq \bar{r}_{m,k}, \ m \in \mathcal{M}, \ k \in \mathcal{K}_m, \tag{17c}$$

where $\hat{R}^{(\kappa)}_{total}\left(\boldsymbol{p}_0\right) = \sum_{m=1}^{M}\sum_{k=1}^{K_m}\hat{R}^{(\kappa)}_{m,k}\left(p_{m,k}\right)$.

Finally, we solve (17) by CVX tools [24] following the Algorithm 1. Particularly, we set up the values of $i = 0$, $\mathbf{\Phi}_M$, and $\varepsilon = 10^{-3}$. The number of iterations is $I_{max} = 20$. The output is the optimal power control coefficients $(\boldsymbol{p}_0^*)$.

Algorithm 1. Power allocation procedure

Input:
$i = 0$, $\mathbf{\Phi}_M$, $\varepsilon = 10^{-3}$
$I_{max} = 20$
while (Divergence or $i \leqslant I_{max}$)
Solve (17) for ($\boldsymbol{p}_0^{(i+1)}$) by CVX
$i = i + 1$
end while
Output: $\boldsymbol{p}_0^*$

4.2 RIS Phase Shift Optimization

With the considering power control coefficients $\boldsymbol{p}_0$, the problem can be rewritten as

$$\max_{\mathbf{\Phi}_M} R_{total}\left(\mathbf{\Phi}_M\right) \tag{18a}$$

$$\text{s.t.} \quad (12c), (12d). \tag{18b}$$

Let $\boldsymbol{h}_{m,k}^H \mathbf{\Phi}_m \boldsymbol{h}_{0,m} = \psi_m^H \chi_{m,k}$ where $\psi_m = [\psi_m^1, ..., \psi_m^N]^H$ with $\psi_m^n = e^{j\theta_{nm}}$ ($\forall n = 1, 2, ..., N$), $\chi_{m,k} = diag(\boldsymbol{h}_{m,k}^H)\boldsymbol{h}_{0,m}$, and $a_k = P_0/\sigma_k^2$. With $|\psi_m^n|^2 = 1$, the constraint in (12d) becomes the unit-modulus constraint [4]. Then, the problem (18) is equivalently rewritten as

$$\max_{\psi_m,\ m\in\mathcal{M}} \sum_{m=1}^{M}\sum_{k=1}^{K_m} \log_2\left(1 + a_k \psi_m^H \chi_{m,k} \chi_{m,k}^H \psi_m\right) \tag{19a}$$

$$\text{s.t.} \quad \psi_m^H \chi_{m,k} \chi_{m,k}^H \psi_m \geq \left(2^{\bar{r}_{m,k}} - 1\right)/a_k, \tag{19b}$$

$$|\psi_m^n|^2 = 1, \forall n = 1, 2, ..., N,\ m \in \mathcal{M}. \tag{19c}$$

Nevertheless, (19) is non-convex. To make (19) become a convex optimization problem, we first denote $\mathbf{X}_{m,k} = \chi_{m,k}\chi_{m,k}^H$ and $\psi_m^H \mathbf{X}_{m,k} \psi_m = tr\left(\mathbf{X}_{m,k}\psi_m\psi_m^H\right) = tr\left(\mathbf{X}_{m,k}\mathbf{\Psi}_m\right)$ where $\mathbf{\Psi}_m = \psi_m\psi_m^H$ must satisfy $\mathbf{\Psi}_m \succeq \mathbf{0}$ and rank($\mathbf{\Psi}_m$)=1. And then, we relax the rank-one constraint of (19c) [6]. Thus, (19) is rewritten as

$$\max_{\psi_m,\ m\in\mathcal{M}} \sum_{m=1}^{M}\sum_{k=1}^{K_m} \log_2\left(1 + a_k tr\left(\mathbf{X}_{m,k}\mathbf{\Psi}_m\right)\right) \tag{20a}$$

$$\text{s.t.} \quad tr\left(\mathbf{X}_{m,k}\mathbf{\Psi}_m\right) \geq \left(2^{\bar{r}_{m,k}} - 1\right)/a_k, \tag{20b}$$

$$\mathbf{\Psi}_{m(n,n)} = 1, \forall n = 1, 2, ..., N,\ m \in \mathcal{M}, \tag{20c}$$

$$\mathbf{\Psi}_m \succeq \mathbf{0}. \tag{20d}$$

As a result, we can see that problem (20) is a convex semidefinite program (SDP) [4], which can be efficiently solved by using CVX. We proposed BCD-based method to solve problem (20) in Algorithm 2. Specifically, we assign $i = 0$,

$\boldsymbol{p}_0$, $\boldsymbol{f}_{m,k}^{(0)}$, and $\varepsilon = 10^{-3}$. The output of this algorithm is the optimal phase shift ($\boldsymbol{\Phi}_M^*$).

Algorithm 2. Phase shift searching procedure

Input:
  $i = 0$, $\boldsymbol{p}_0$, $\boldsymbol{f}_{m,k}^{(0)}$, $\varepsilon = 10^{-3}$
  $I_{max} = 20$
while (Divergence or $i \leqslant I_{max}$)
  for $m = [1 : M]$
    Solve (20) for ($\boldsymbol{\Phi}_M^{(i+1)}$) by CVX
    $\boldsymbol{f}_{m,k}^{(i+1)}$
  end for
  $i = i + 1$
end while
Output: $\boldsymbol{\Phi}_M^*$

Lastly, the Algorithms 1 and 2 are combined to solve the joint power allocation and phase shifts optimization.

5 Simulation Results

In this section, we investigate simulation results in Matlab to figure out the performance of the proposed method. We consider parameters of simulation as follows. The radius of circle coverage is 500 m. The radius of expanded deployment area is 2000m. In additional, we assume that the BS is located at $(0, 0, 30)$. The white power spectral density and QoS threshold are assigned to $\sigma^2 = -130$ dBm/Hz and $\bar{r}_{m,k} = 1$ bps/Hz, respectively. In term of the channel model, we set up the same as the settings in [23,25]. We conduct numerical results from our proposed method as in (12) i.e., optimal power allocation - optimal phase shift (OP-OPH), and the conventional methods i.e., optimal power allocation - random phase shift (OP-RPH), equal power allocation - random phase shift (EP-OPH), and equal power allocation - random phase shift (EP-RPH).

In Fig. 2 and Fig. 3, the total network throughput is plotted in two scenarios with the number of reflecting elements is fixed $N = 50$. In Fig. 2, we assume that the number of RISs and the number of UEs are $M = 4$ and $K = 20$, respectively. The number RISs is $M = 8$ and the number of UEs is $K = 30$ in Fig. 3. It is clear that the total network throughput rises when the transmit power at the BS increases. Specifically, when the number of RISs is increased, the total network throughput rises considerably. Moreover, in the consider method, the optimal phase shift can be more efficient than the others in all scenarios in Fig. 2 and Fig. 3.

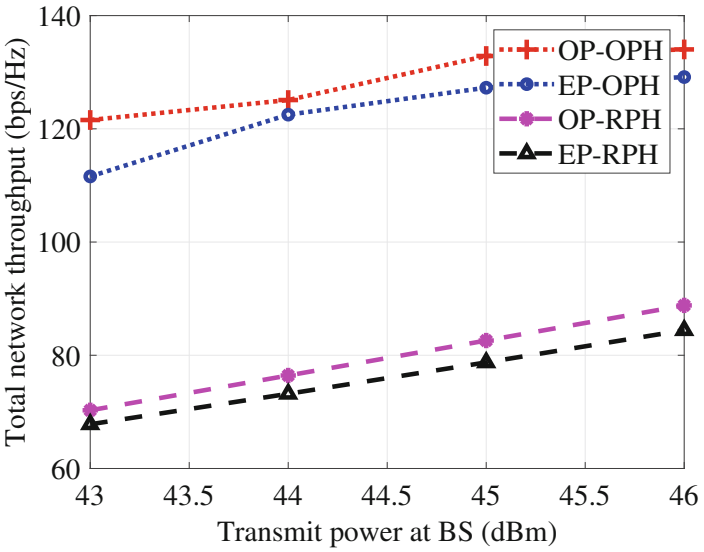

Fig. 2. Total throughput versus number of RISs ($M = 4$, $K = 20$, $N = 50$).

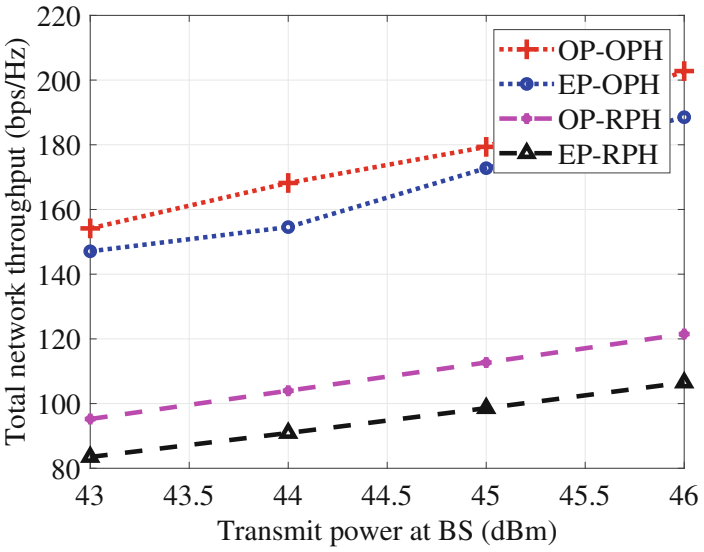

Fig. 3. Total throughput versus transmission power at BS ($M = 8$, $K = 30$, $N = 50$).

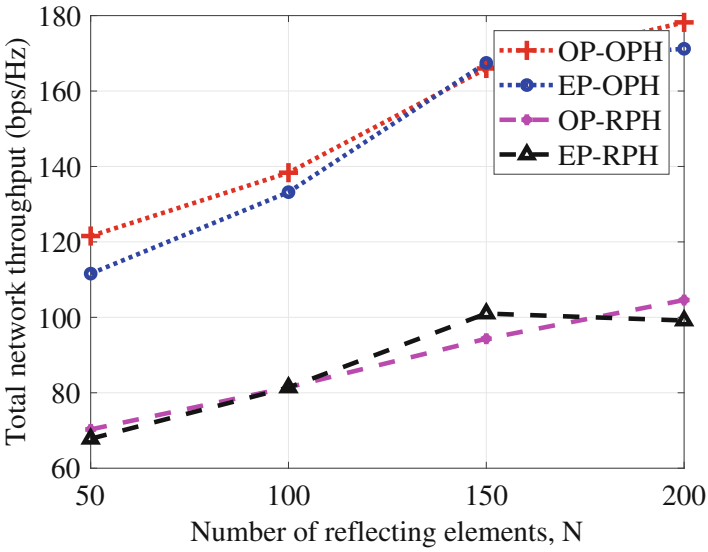

Fig. 4. Total throughput versus number of reflecting elements ($M = 4$, $K = 20$, $P_0^{\max} = 43$ dBm).

Meanwhile, we illustrate the total network throughput versus different of RIS elements when $M = 4$, $K = 20$, and $P_0^{\max} = 43$ dBm in Fig. 4. Clearly, as can be seen that the total network throughput grows steadily when the number of reflecting elements rises. In particular, the result shows that the total network throughput of proposed network is significantly larger than others in case the phase shift is optimized. As expected, the OP-OPH is the best method for RIS-aided downlink cellular network. Despite the fact that $P_0^{\max}$ is fixed to 43 dBm, the OP-OPH method can achieve approximately much more 1,8 times than the EP-RPH method.

Finally, in case of the number of RIS $M = 4$, the number of user $K = 20$, and $P_0^{\max} = 43$ dBm, the results in Fig. 2 and Fig. 4 prove that the total network throughput heightens about 1,5 times when we increase the number of reflecting elements from $N = 50$ to $N = 200$.

6 Conclusions

In this paper, we have studied the assistance of RIS for downlink cellular networks. Aiming to enhance the QoS of cellular network, the joint power allocation coefficients of BS and phase shifts of RIS optimization was applied. The numerical results demonstrated the efficiency of proposed system. The total network throughput achieved the highest in case both power and phase shift are optimized. Obviously, the coverage is expanded thanks to the RIS assisted, but not investigated in this paper.

References

1. Basar, E., Di Renzo, M., De Rosny, J., Debbah, M., Alouini, M.-S., Zhang, R.: Wireless communications through reconfigurable intelligent surfaces. IEEE Access **7**, 116753–116773 (2019)
2. Wu, Q., Zhang, S., Zheng, B., You, C., Zhang, R.: Intelligent reflecting surface-aided wireless communications: a tutorial. IEEE Trans. Commun. **69**(5), 3313–3351 (2021)
3. Wu, Q., Zhang, R.: Towards smart and reconfigurable environment: intelligent reflecting surface aided wireless network. IEEE Commun. Mag. **58**(1), 106–112 (2020)
4. Wu, Q., Zhang, R.: Intelligent reflecting surface enhanced wireless network via joint active and passive beamforming. IEEE Trans. Wireless Commun. **18**(11), 5394–5409 (2019)
5. Huang, K.-W., Wang, H.-M.: Passive beamforming for IRS aided wireless networks. IEEE Wireless Commun. Lett. **9**(12), 2035–2039 (2020)
6. Yu, H., Tuan, H.D., Nasir, A.A., Duong, T.Q., Poor, H.V.: Joint design of reconfigurable intelligent surfaces and transmit beamforming under proper and improper gaussian signaling. IEEE J. Sel. Areas Commun. **38**(11), 2589–2603 (2020)
7. Li, S., Duo, B., Yuan, X., Liang, Y.-C., Di Renzo, M.: Reconfigurable intelligent surface assisted UAV communication: joint trajectory design and passive beamforming. IEEE Wireless Commun. Lett. **9**(5), 716–720 (2020)
8. Nguyen, K.K., Khosravirad, S., da Costa, D.B., Nguyen, L.D., Duong, T.Q.: Reconfigurable Intelligent Surface-assisted Multi-UAV Networks: Efficient Resource Allocation with Deep Reinforcement Learning (2021)
9. Nguyen, K.K., Masaracchia, A., Yin, C., Nguyen, L.D., Dobre, O.A., Duong, T.Q.: Deep Reinforcement Learning for Intelligent Reflecting Surface-Assisted D2D Communications (2021)
10. Ha, D.-B., Truong, V.-T., Lee, Y.: Performance analysis for RF energy harvesting mobile edge computing networks with SIMO/MISO-NOMA schemes. EAI Endorsed Trans. Ind. Netw. Intell. Syst. **8**(27), 4 (2021)
11. Fang, F., Xu, Y., Pham, Q.-V., Ding, Z.: Energy-efficient design of IRS-NOMA networks. IEEE Trans. Veh. Technol. **69**(11), 14088–14092 (2020)
12. Zhang, D., Wu, Q., Cui, M., Zhang, G., Niyato, D.: Throughput maximization for IRS-assisted wireless powered hybrid NOMA and TDMA. IEEE Wireless Commun. Lett. **10**(9), 1944–1948 (2021)
13. Wu, Q., Zhang, R.: Joint active and passive beamforming optimization for intelligent reflecting surface assisted SWIPT under QoS constraints. IEEE J. Sel. Areas Commun. **38**(8), 1735–1748 (2020)
14. Mu, X., Liu, Y., Guo, L., Lin, J., Al-Dhahir, N.: Exploiting intelligent reflecting surfaces in NOMA networks: joint beamforming optimization. IEEE Trans. Wireless Commun. **19**(10), 6884–6898 (2020)
15. Wu, Q., Zhang, R.: Weighted sum power maximization for intelligent reflecting surface aided SWIPT. IEEE Wireless Commun. Lett. **9**(5), 586–590 (2020)
16. Guo, H., Liang, Y.-C., Chen, J., Larsson, E.G.: Weighted sum-rate maximization for intelligent reflecting surface enhanced wireless networks. In: IEEE Global Communications Conference (GLOBECOM) 2019, pp. 1–6 (2019)
17. Nguyen, M., Nguyen, L.D., Duong, T.Q., Tuan, H.D.: Real-time optimal resource allocation for embedded UAV communication systems. IEEE Wireless Commun. Lett. **8**(1), 225–228 (2019)

18. Bor-Yaliniz, R.I., El-Keyi, A., Yanikomeroglu, H.: Efficient 3-D placement of an aerial base station in next generation cellular networks. In: IEEE ICC, pp. 1–5, May 2016
19. Mozaffari, M., Saad, W., Bennis, M., Debbah, M.: Efficient deployment of multiple unmanned aerial vehicles for optimal wireless coverage. IEEE Commun. Lett. **20**, 1647–1650 (2016)
20. Al-Hourani, A., Kandeepan, S., Lardner, S.: Optimal LAP altitude for maximum coverage. IEEE Wireless Commun. Lett. **3**(6), 569–572 (2014)
21. Xie, X., Fang, F., Ding, Z.: Joint optimization of beamforming, phase-shifting and power allocation in a multi-cluster IRS-NOMA network. IEEE Trans. Veh. Technol. **70**(8), 7705–7717 (2021)
22. Wu, Q., Zhang, R.: Beamforming optimization for wireless network aided by intelligent reflecting surface with discrete phase shifts. IEEE Trans. Commun. **68**(3), 1838–1851 (2020)
23. Nguyen, L.D., Tuan, H.D., Duong, T.Q., Dobre, O.A., Poor, H.V.: Downlink beamforming for energy-efficient heterogeneous networks with massive MIMO and small cells. IEEE Trans. Wireless Commun. **17**(5), 3386–3400 (2018)
24. Grant, M., Boyd, S.: CVX: MATLAB software for disciplined convex programming, version 2.1, March 2014. http://cvxr.com/cvx
25. Do-Duy, T., Nguyen, L.D., Duong, T.Q., Khosravirad, S., Claussen, H.: Joint optimisation of real-time deployment and resource allocation for UAV-aided disaster emergency communications. IEEE J. Sel. Areas Commun. **39**(11), 3411–3424 (2021)